Quaternary Research (2017), **87**, 180–189.

doi:10.1017/qua.2016.7

Comparative ^{14}C and OSL dating of loess-paleosol sequences to evaluate post-depositional contamination of *n*-alkane biomarkers

Michael Zech[a,b*,1], Sebastian Kreutzer[b,c,2], Roland Zech[d,3], Tomasz Goslar[e], Sascha Meszner[f], Cameron McIntyre[d,4], Christoph Häggi[d,5], Timothy Eglinton[d], Dominik Faust[f], Markus Fuchs[c]

[a]Institute of Agronomy and Nutritional Sciences, Soil Biogeochemistry, Martin-Luther-Universität Halle-Wittenberg, Von-Seckendorff-Platz 3, 06120 Halle (Saale), Germany
[b]Department of Geomorphology and Department of Soil Physics, University of Bayreuth, Universitätsstr. 30, 95440 Bayreuth, Germany
[c]Department of Geography, Justus-Liebig-University Giessen, Senckenbergstr. 1, 35390 Giessen, Germany
[d]Geological Institute, Biogeoscience Group, ETH Zurich, Sonneggstr. 5, 8092 Zurich, Switzerland
[e]Poznan Radiocarbon Laboratory, ul. Rubiez 46, 61-612 Poznan, Poland
[f]Department of Geography, Chair of Physical Geography, Dresden University of Technology, Helmholtzstr. 10, 01069 Dresden, Germany

(Received April 19, 2016; Accepted November 1, 2016)

Abstract

There is an ongoing controversial discussion as to whether *n*-alkane lipid biomarkers—and organic matter of loess in general—reflect a synsedimentary paleoenvironmental/climate signal or whether they are significantly affected by postdepositional "contamination," for example related to root and rhizomicrobial activity. In order to address this issue at our study site (the Middle to Late Weichselian loess-paleosol sequence Gleina in Saxony, Germany), we determined and compared radiocarbon ages of bulk *n*-alkanes and sedimentation ages, as assessed by optically stimulated luminescence (OSL) dating. The bulk *n*-alkanes of the four dated samples yielded calibrated ^{14}C ages ranging from 24.1 to 49.7 cal ka BP (95.4% probability ranges). While the three uppermost *n*-alkane samples are well within the range or even slightly older than the OSL-inferred sedimentation ages, the lowermost *n*-alkane sample is slightly younger than the OSL ages. There is hence little or no evidence at our study site for *n*-alkanes in loess-paleosol sequences being significantly "contaminated" by deep subsoil rooting or microbial processes. We propose a ^{14}C isotope mass balance calculation for estimating such contaminations quantitatively. Radiocarbon dating of bulk *n*-alkanes might have great potential for Quaternary research, and we encourage further comparative ^{14}C and OSL studies.

Keywords: Loess; Subsoil; Soil organic matter; Lipid biomarkers; *n*-Alkanes; Roots; Rhizomicrobial; Luminescence dating; Radiocarbon dating

INTRODUCTION

Loess-paleosol sequences (LPSs) are important terrestrial archives for reconstructing Quaternary climate and landscape history (e.g., Zöller and Faust, 2009; Frechen, 2011; Marković et al., 2011; Stevens et al., 2011; Antoine et al., 2013; Kadereit et al., 2013; Meszner et al., 2013). Although biomarkers have been proved for decades to be of outstanding value as molecular fossils in marine and lacustrine sediments (Eglinton and Eglinton, 2008), they have been much less investigated in LPSs (for a review see, e.g., Zech et al., 2011b). This has several reasons, among

*Corresponding author at: Institute of Agronomy and Nutritional Sciences, Soil Biogeochemistry, Martin-Luther-Universität Halle-Wittenberg, Von-Seckendorff-Platz 3, 06120 Halle (Saale), Germany. E-mail address: michael_zech@gmx.de (M. Zech).

[1] Present address: Department of Geography, Chair of Landscape- and Geoecology, Faculty of Environmental Sciences, Dresden University of Technology, Helmholtzstr. 10, 01062 Dresden, Germany.

[2] Present address: IRAMAT-CRP2A, Université Bordeaux Montaigne, Maison de l'Archéologie, Esplanade des Antilles, 33607 Pessac Cedex, France.

[3] Present address: Institute of Geography and Oeschger Centre for Climate Change Research, Biogeochemistry and Paleoclimatology Group, University of Bern, Hallerstr. 12, 3012 Bern, Switzerland.

[4] Present address: Scottish Universities Environmental Research Centre (SUERC), Rankine Avenue, Scottish Enterprise Technology Park, East Kilbride, G750QF, Glasgow, United Kingdom.

[5] Present address: MARUM – Center for Marine Environmental Sciences, University of Bremen, Leobener Str., 28359 Bremen, Germany.

others, but primarily is because of the generally very low concentration of organic matter (OM) in loess.

Only during the last decade, plant leaf wax–derived lipids, particularly long-chain *n*-alkanes, have come into focus for organic geochemists using LPSs as paleoenvironmental/climate archives (Xie et al., 2002, 2003; Zhang et al., 2006; Bai et al., 2009). The popularity of *n*-alkanes as biomarkers can be attributed to the relatively easy procedure to extract and analyze them in the laboratory, as well as their recalcitrance and good preservation in loess. This allows results to be obtained even from loess samples with low organic content. Furthermore, *n*-alkanes can be used to infer vegetation changes in terms of grasses (dominated by the *n*-alkane homologues nC_{31} and nC_{33}) versus deciduous trees (dominated by the *n*-alkane homologues nC_{27} and nC_{29}) (Kirkels et al., 2013; Schäfer et al., 2016b). It may be noteworthy that soil microbial degradation can affect *n*-alkane patterns and may need to be considered in certain cases (Zech et al., 2009; Buggle et al., 2010; Nguyen Tu et al., 2011; Zech et al., 2013a; Schäfer et al., 2016a). Last but not least, the compound-specific hydrogen isotope (δ^2H) signature of *n*-alkanes and its coupling with the compound-specific oxygen isotope ($\delta^{18}O$) signature of hemicellulose-derived sugar biomarkers are emerging as highly innovative paleoclimate tools in loess research (Liu and Huang, 2005; Zech et al., 2013b, 2013c).

A major and crucial assumption of all paleoreconstructions based on *n*-alkanes, as well as on any other biomarker in loess, is that the *n*-alkanes are deposited synsedimentarily and are not "contaminated" significantly by postdepositional processes. This issue, however, has been highly disputed for several years (Wiesenberg, 2012 vs. Zech et al., 2012a; Wiesenberg and Gocke, 2013 vs. Zech et al., 2012b; Gocke and Wiesenberg, 2013 vs. Häggi et al., 2014). Gocke et al. (2010, 2013, 2014) claimed that a significant overprinting of loess OM, including *n*-alkanes, occurred during the Holocene and still occurs in modern times by deep subsoil rooting and rhizomicrobial deposition even in loess distant to former roots. Given that the interpretation of *n*-alkane biomarker patterns alone is not straightforward for reconciling this controversy, comparative ^{14}C and optically stimulated luminescence (OSL) dating can serve as an elegant alternative approach. Postdepositional root/rhizomicrobial contamination would result in a rejuvenation of the synsedimentary leaf wax–derived *n*-alkanes in loess. OSL, by comparison, yields (synsedimentary) sedimentation ages. Although ^{14}C dating of *n*-alkanes has already been proved to be a powerful tool in soil science and marine sediments (Lichtfouse and Eglinton, 1995; Huang et al., 1999; Kusch et al., 2010), this method has until now rarely been applied in loess research. Only recently, Häggi et al. (2014) performed compound-specific ^{14}C dating of individual *n*-alkane homologues after gas chromatography (GC) separation on a preparative GC. They found the *n*-alkanes to yield ^{14}C ages that agree well with the luminescence ages for the investigated LPS Crvenka in Serbia. However, those results are still awaiting verification from other sites, and compound-specific ^{14}C dating is very laborious. This latter disadvantage may be overcome by ^{14}C dating of purified bulk *n*-alkane fractions (Haas et al., 2016).

The aim of this study was therefore to evaluate the potential of bulk, rather than compound-specific, *n*-alkane ^{14}C dating for answering the question of whether *n*-alkane biomarkers in loess are primarily synsedimentary or whether they are significantly contaminated by root/rhizomicrobial OM. Bulk *n*-alkanes were extracted, purified, and dated for the Middle to Late Weichselian LPS Gleina in Saxony, Germany. The sedimentation ages were assessed by OSL dating; therefore the methodological limits of this approach need to be kept in mind (i.e., possible age under- or overestimation because of postdepositional sediment mixing or insufficient bleaching). We propose a ^{14}C isotope mass balance calculation to estimate the potential postdepositional root/rhizomicrobial contamination quantitatively.

MATERIAL AND METHODS

The LPS Gleina

Loess and paleosol samples were collected from the LPS Gleina (51°13.83N, 13°14.55E), which is located in the Saxon loess region, eastern Germany (Lieberoth, 1963; Haase et al., 1970; Meszner et al., 2011). A detailed description of the stratigraphy was provided by Meszner et al. (2011). In brief, the uppermost meter is composed of decalcified material representing the Holocene pedogenetic impact. Major parts of the Holocene soil (Luvisol) are truncated, and a plough horizon (Ap horizon) nowadays forms the topsoil. According to the pan-European loess stratigraphic model suggested by Marković et al. (2015), this unit refers to S0. Below, down to approximately 8 m depth and referring to L1LL1 according to Marković et al. (2015), six paleosols, which can be described as fossil gelic gleysols and fossil brown tundra gleysols, alternate with loess layers (Fig. 1A). From approximately 8 m on, there is strong evidence for accumulation of partly reworked material. In situ pedogenesis contributed to the formation of a fossil gelic gleysol at approximately 8.5 m depth and to the formation of the decalcified so-called Gleina complex (defined by Lieberoth [1963] and Meszner et al. [2013] and referring to L1SS1 according to Marković et al. [2015]) at approximately 10 m depth. The underlying so-called Lommatzsch soil complex (Lieberoth, 1963) was sampled from a nearby profile (approximately 20 m away) and is separated in Figure 1 by an unconformity.

Modern root contamination partly occurred in the upper 4.5 m of the sequence, whereas hardly any modern roots were found in the lower part of the sequence. The risk of modern lateral root contamination was minimized by setting back the exposure wall by at least half a meter over the whole height of the exposure. Few rhizoliths, presumably documenting a Holocene root contamination, were found in the fossil gelic gleysol at 2 m depth.

n-Alkane preparation, radiocarbon dating, and quantification of postdepositional *n*-alkane contamination by roots

For radiocarbon dating of the bulk *n*-alkanes, four samples were selected from the Gleina LPS, for which *n*-alkane concentrations and patterns were already investigated and

https://doi.org/10.1017/qua.2016.7 Published online by Cambridge University Press

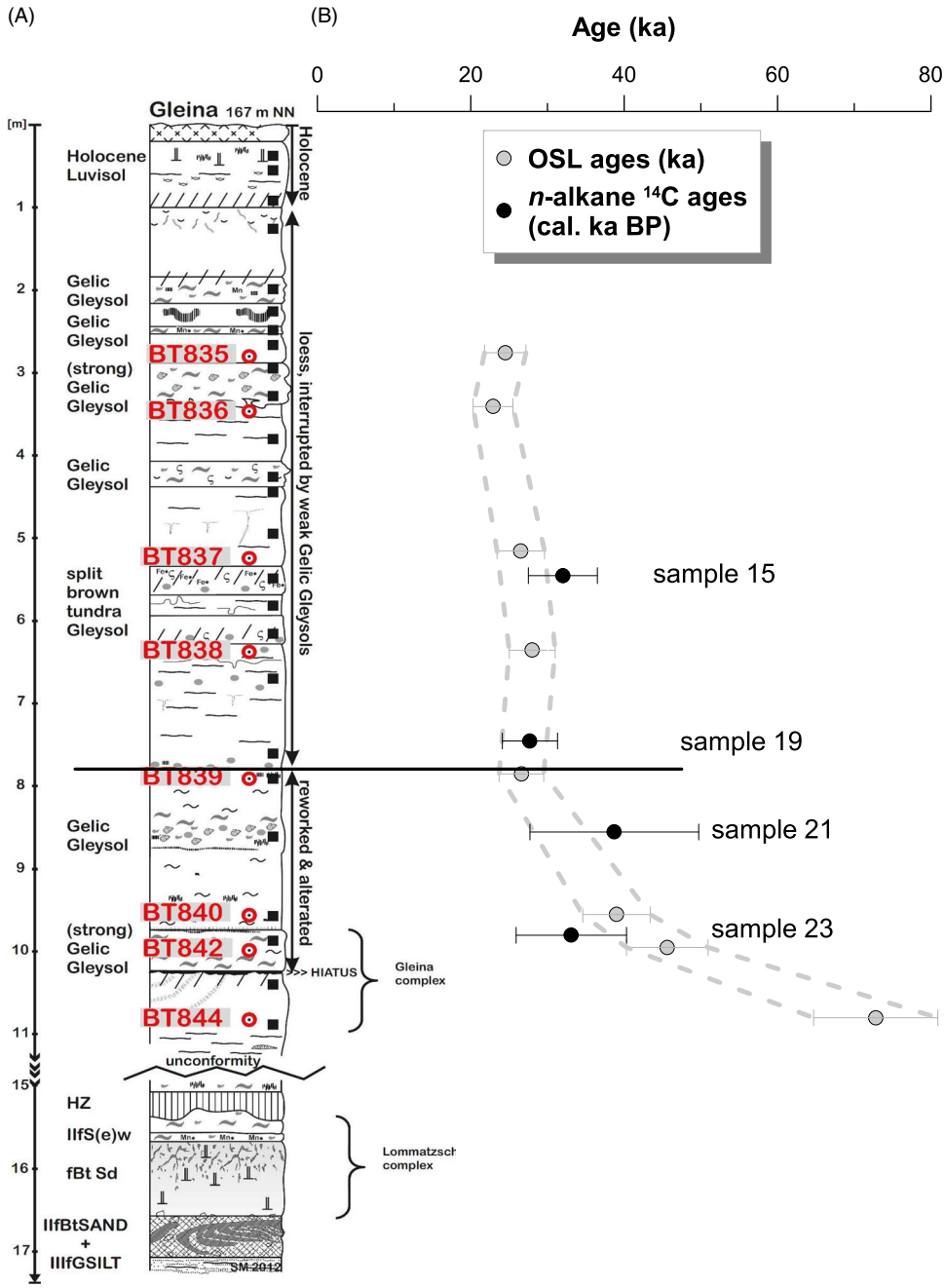

Figure 1. (color online) (A) Stratigraphy of the loess-paleosol sequence Gleina. Red numbers on the stratigraphic column and filled black squares, respectively, mark the position of the optically stimulated luminescence (OSL) and *n*-alkane samples. (B) Age-depth profiles of calibrated ^{14}C bulk *n*-alkane ages (95.4% probability ranges) and OSL ages with their 2σ error bars.

published (Zech et al., 2013a; cf. fig. 1 therein). The samples were chosen according to their *n*-alkane concentrations (sum of long-chain *n*-alkanes >3 µg/g) and their stratigraphic position. While the samples 15 and 19 represent a weakly developed gleysol and a loess unit, respectively, from the upper part of the Gleina section (with no signs of reworking), samples 21 and 23 represent a weakly and a strongly developed gleysol, respectively, from the lower reworked part of the Gleina section (Fig. 1). For comparison, two approximately 160 ka old samples from LPS Tumara, northeast Siberia (Zech et al., 2010), and a modern litter sample were analyzed as radiocarbon dead and modern reference materials, respectively (Table 1).

The *n*-alkane preparation followed the procedure described by Häggi et al. (2014). In brief, free lipids were obtained with a Dionex ASE 200 accelerated solvent extractor using dichloromethane and methanol. *n*-Alkanes were purified and eluted over aminopropyl columns. Subsequent further purification steps involved $AgNO_3$ and zeolite (Geokleen) pipette columns (McDuffee et al., 2004) and served to obtain as clean bulk *n*-alkane fractions as possible (chromatograms are shown in Fig. 2). Radiocarbon measurements were

https://doi.org/10.1017/qua.2016.7 Published online by Cambridge University Press

Table 1. Results of radiocarbon analyses for the purified bulk *n*-alkane fractions of reference materials and four investigated samples from the loess-paleosol sequence Gleina.

Sample name	Lab code	Material: purified bulk *n*-alkanes from	µg C	$\delta^{13}C$ (‰)	Measured $F^{14}C$	Error	Corrected[a] $F^{14}C$	Error[b]	^{14}C age (ka BP)	Error (ka)	Calibrated age[c] (cal ka BP)
Sample 12/9x	ETH 53126.1.1	~160 ka old sediments	42.9	–20.0	0.0136	0.0009	0.0072	0.0145[d]	>28.4	n.a.	n.a.
Sample 12/9j	ETH 53127.1.1		30.3	–24.1	0.0118	0.0010	0.0025	0.0269[d]	>23.5	n.a.	n.a.
Sample 5L	ETH 53129.1.1	Modern litter	45.7	–20.8	1.0205	0.0092	1.0234	0.0094	–0.2	0.1	n.a.
Sample 15	ETH 53125.1.1	Gleina loess-paleosol sequence	36.4	–20.4	0.0442	0.0014	0.0366	0.0078	26.6	1.9	27.5–36.5
Sample 19	ETH 53124.1.1		25.9	–32.0	0.0680	0.0022	0.0581	0.0106	22.9	1.6	24.1–31.2
Sample 21	ETH 53122.1.1		26.9	–29.9	0.0387	0.0016	0.0284	0.0142	28.6	5.6	27.7–49.7
Sample 23	ETH 53123.1.1		28.8	–27.3	0.0482	0.0017	0.0391	0.0105	26.0	2.5	26.0–40.3

[a]Corrected for a vacuum line combustion blank of 0.4 ± 0.1 µg C with an $F^{14}C$ of 0.7 ± 0.2.
[b]Error propagation after Shah and Pearson (2007).
[c]Calibration done with OxCal 4.2 and the IntCal13 calibration curve (Bronk Ramsey, 2009; Reimer et al., 2013).
[d]Relative error >50%. Therefore, according to convention, minimum ages were not calculated using the corrected $F^{14}C$ value, but twice the absolute error.

conducted on an accelerator mass spectrometer (MICADAS, Ionplus) system at the Laboratory for Ion Beam Physics, ETH Zurich. Radiocarbon ages were converted to calendar ages using OxCal 4.2 (Bronk Ramsey, 2009) and the IntCal13 calibration curve (Reimer et al., 2013). Calibrated ^{14}C ages (cal ka BP) are provided as 95.4% probability range in Table 1 and Figure 1B. All bulk *n*-alkane radiocarbon data were corrected for a vacuum line combustion blank of 0.4 ± 0.1 µg C with a fraction of modern carbon ($F^{14}C$) of 0.7 ± 0.2 (Table 1) using an isotope mass balance according to Shah and Pearson (2007).

$$F^{14}C_{corrected} = \frac{\left(F^{14}C_{uncorrected} \times mass_{sample}(\text{in µgC}) - 0.7 \times 0.4\right)}{mass_{sample}(\text{in µgC}) - 0.4} \quad \text{(Eq. 1)}$$

OSL dating

A numerical chronostratigraphy of the Gleina section was established by OSL dating using fine-grain (4–11 µm) quartz separates. Eight luminescence samples, generally from loess below or above paleosols and covering the depth from 2.9 to 10.8 m, were taken during nighttime and prepared in the laboratory for equivalent dose (D_e) determination using standard methods for fine-grain quartz dating (e.g., Fuchs et al., 2005). The OSL measurements were carried out on Risø TL/OSL DA-15 luminescence readers using blue light stimulation (470 Δ 30 nm). Signals were detected in the UV band (340 Δ 80 nm). For D_e determination on 12 aliquots per sample, a standard single aliquot regenerative (SAR) protocol according to Murray and Wintle (2000) was applied using the first 0.2 s after subtracting the background from the last 4 s of the shine-down curves. SAR protocol parameters were previously deduced from test measurements, and the purity of the quartz extracts was tested by infrared light stimulation. The mean D_e and its standard error for each sample were used for age calculation. For dose rate calculation, the U, Th, and K concentrations were measured using inductively coupled plasma mass spectrometry (K) and thick source alpha counting (e.g., Zöller and Pernicka, 1989). The α-effectiveness (*a*-value) was measured for each sample following the procedure described in Mauz et al. (2006) and Lai et al. (2008) and resulted in a mean *a*-value of 0.04 with a standard deviation of 0.01 (n = 8; cf. Supplementary Table 1). The cosmic dose rate was calculated according to Prescott and Hutton (1994). A water content of 20% ± 5% was used. Further methodological details on the luminescence dating are given in the Supplementary Materials.

RESULTS AND DISCUSSION

n-Alkane patterns

The *n*-alkane chromatograms of the four ^{14}C-dated *n*-alkane samples reveal a bimodal pattern (Fig. 2). The long-chain *n*-alkanes (>nC_{25}) are characterized by a high odd-over-even predominance; that is, particularly the *n*-alkanes nC_{27}, nC_{29}, nC_{31}, and nC_{33} are by far more abundant than the *n*-alkanes

https://doi.org/10.1017/qua.2016.7 Published online by Cambridge University Press

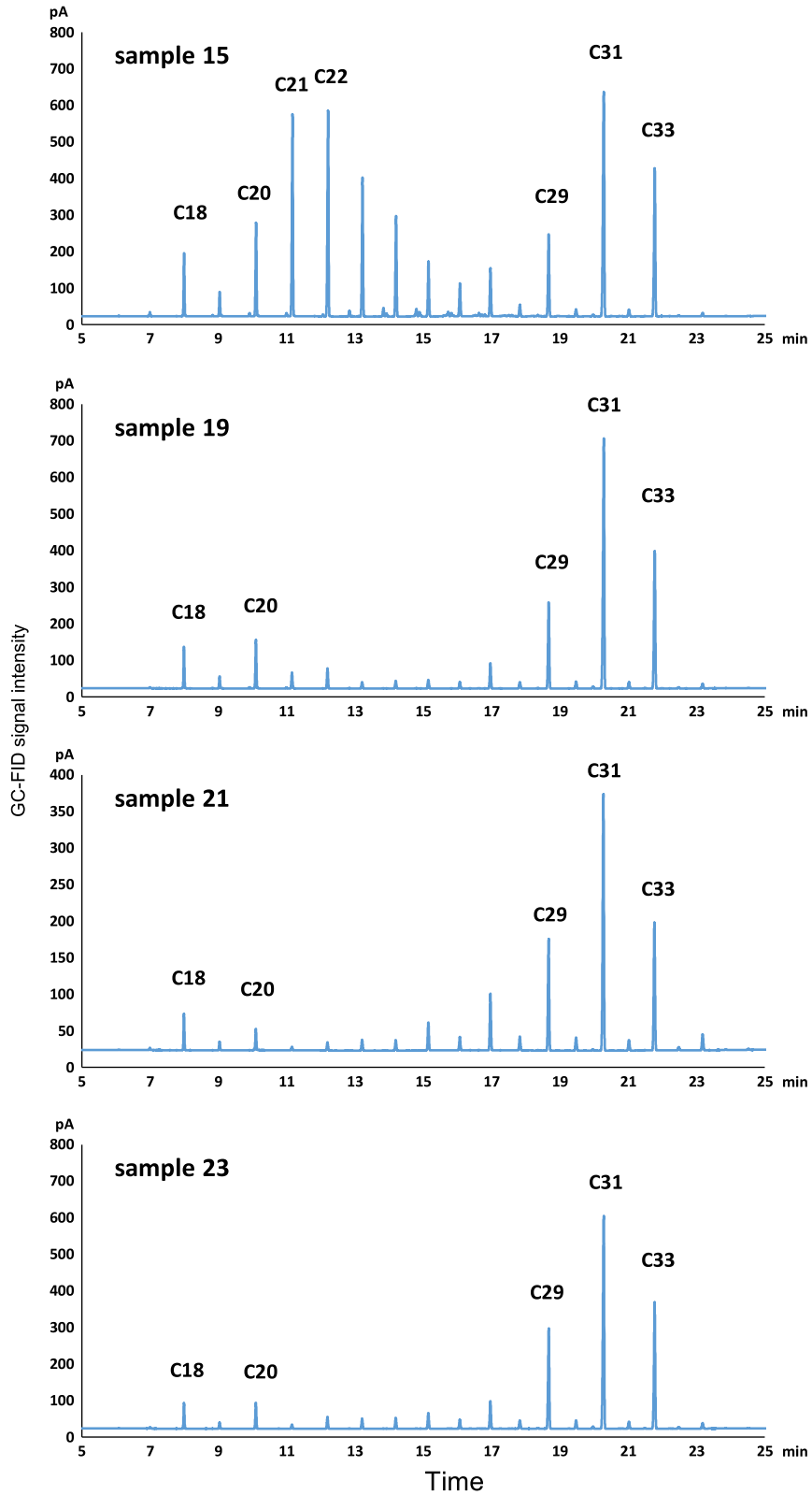

Figure 2. (color online) GC-FID (gas chromatography - flame ionisation detector) *n*-alkane chromatograms for the four radiocarbon-dated bulk *n*-alkane samples. The x-axes represent the retention time in minutes; the y-axes represent the GC-FID signal intensity in picoamperes. The long-chain *n*-alkanes nC_{29}, nC_{31}, and nC_{33} originate from plant leaf waxes; the nC_{31} dominance indicates dominant grass orgin; potential sources of short- and midchained *n*-alkanes nC_{18}, nC_{20}, nC_{21}, and nC_{22} are charred and soil microbial biomass.

https://doi.org/10.1017/qua.2016.7 Published online by Cambridge University Press

nC_{28}, nC_{30}, and nC_{32}. Such patterns are typical for leaf wax–derived *n*-alkanes (Eglinton and Hamilton, 1967; Kolattukudy, 1976). The dominance of nC_{31} indicates that grasses were the main source (Maffei, 1996; Zech et al., 2013a; Schäfer et al., 2016b). The compounds nC_{18} and nC_{20} also occur in relatively high amounts, and in sample 15, additionally nC_{21} and nC_{22} (Fig. 2). While these *n*-alkanes typically do not or rarely occur in higher plant leaf waxes (Kuhn et al., 2010), Wiesenberg et al. (2009) showed that charring of grass biomass at 400°C to 500°C produces such *n*-alkane patterns. Soil microorganisms are reported to produce short- and midchained *n*-alkanes as well (Grimalt and Albaigés, 1987; Buggle et al., 2010; Zech et al., 2011a). We hence conclude that apart from plant leaf waxes, charred biomass and soil microbial biomass also likely contributed to the investigated *n*-alkane fractions with short-chained *n*-alkanes serving as respective molecular markers.

^{14}C ages of the bulk n-alkane samples

Radiocarbon dating of the bulk *n*-alkane fractions of the two approximately 160 ka old samples from the LPS Tumara (Zech et al., 2010) yielded very low blank-corrected $F^{14}C$ values of 0.0072 and 0.0025 (Table 1). However, because of the error propagation after Shah and Pearson (2007), the absolute errors are relatively large (0.0145 and 0.0269, respectively, resulting in relative errors >50%). According to convention, minimum ages were therefore not calculated using the corrected $F^{14}C$ values, but twice the absolute errors (Table 1), which yielded ^{14}C *n*-alkane minimum ages of >28.4 and >23.5 ka BP. For comparison, the modern litter sample yielded a corrected $F^{14}C$ value of 1.0234, corresponding to a ^{14}C *n*-alkane age of −185 ± 75 yr BP (Table 1). Thus, the ^{14}C *n*-alkane results of the radiocarbon dead and modern reference materials corroborate the reliability of the bulk *n*-alkane ^{14}C analyses performed here.

The bulk *n*-alkanes of the four dated loess-paleosol samples from the LPS Gleina yielded blank-corrected $F^{14}C$ values ranging from 0.028 to 0.058. This corresponds to calibrated ^{14}C ages of 32.0 ± 4.5 cal ka BP, 27.2 ± 3.6 cal ka BP, 38.7 ± 11.0 cal ka BP, and 33.1 ± 7.2 cal ka BP for the samples 15, 19, 21, and 23, respectively. Although the midvalues suggest the occurrence of chronostratigraphic inconsistencies or age inversions (Fig. 1B), the large 95.4% probability ranges, which are calculated according to the error propagation method of Shah and Pearson (2007) and which have to be taken into account, actually do not support this first impression.

OSL ages and establishment of a chronostratigraphy for the Gleina LPS

OSL fine-grain quartz ages and their D_e values are shown in Table 2 and Figure 1. Age results are given as mean and 2σ standard error. All age values consistently increase with profile depth, and within error no age inversion occurred. The quartz luminescence signals were bright, fast decaying, and highly reproducible for the determined preheat and dose recovery tests. For all samples, no significant feldspar contamination (infrared-stimulated luminescence/OSL <1%) was detected. Consequently, the derived D_e distributions show narrow scatters ($c_v \sim 5\%$). The dose rate (Supplementary Materials) varies between 3.1 ± 0.2 Gy/ka (BT836) and 3.5 ± 0.2 Gy/ka (BT842) showing typical values for loess deposits from this region (e.g., Kreutzer et al., 2012).

Table 2. Optically stimulated luminescence quartz fine-grain age estimates.

Sample	Depth (m)	n	Fit	D_e (Gy)	Age (ka)
BT835	2.9	12/12	EXP+LIN	80.4 ± 0.69	24.5 ± 2.7
BT836	3.4	12/12	EXP+LIN	71.04 ± 1.14	22.9 ± 2.6
BT837	5.3	12/12	EXP+LIN	89.73 ± 1.72	26.5 ± 3.1
BT838	6.2	12/12	EXP+LIN	88.17 ± 0.92	28.0 ± 3.0
BT839	7.9	12/12	EXP+LIN	87.71 ± 0.99	26.6 ± 2.9
BT840	9.8	12/12	EXP+LIN	132.91 ± 1.33	39.0 ± 4.4
BT842	10	12/12	EXP+LIN	161.38 ± 1.25	45.6 ± 5.3
BT844	10.8	12/12	EXP+LIN	235.46 ± 2.41	72.8 ± 8.1

Note: Ages given as mean with 2σ uncertainty.

For the uppermost part of the profile (~3 m up to ~8 m), ages between 24.5 ± 2.7 ka (BT835) and 26.6 ± 2.9 ka (BT839) indicate rapid eolian deposition during marine isotope stage 2 (MIS2; Lisiecki and Raymo, 2005). These results are in accordance with previous findings from the Saxonian loess region (Meszner et al., 2011, 2013; Kreutzer et al., 2012). The onset of loess sedimentation at ~10 m was attributed to the MIS3 (BT842: 45.6 ± 5.3 ka; BT840: 39.0 ± 4.4 ka). Below a hiatus at ~10.2 m, the sediment was dated to the early Weichselian (72.8 ± 8.1 ka BT844, MIS5a to MIS4). This hiatus has been observed for all investigated loess profiles in the Saxonian loess region. In contrast to other investigated loess profiles in Saxony (Ostrau, Seilitz: Kreutzer et al., 2012; Meszner et al., 2013), where the onset of loess sedimentation has been dated to ca. 30 ka (transition MIS3 to MIS2), the Gleina loess OSL ages reveal an onset of loess deposition earlier in MIS3. These findings may indicate locally favored loess accumulation and preservation because of its special topographic position on the northernmost boundary of loess distribution in the Saxonian loess region. However, although unlikely in our case, an age overestimation as a result of an incomplete signal resetting during secondary translocation processes cannot be fully excluded, because it is not possible to detect any incomplete signal resetting using fine-grain quartz dating. Although great care was taken during sampling, an age underestimation because of postdepositional mixing by bioturbation might add some uncertainty with regard to interpreting the luminescence ages. The previously described processes have opposite effects and might cancel each other out, and we consider them as being covered by the provided standard errors. Further details on the luminescence dating results are provided in the Supplementary Materials.

https://doi.org/10.1017/qua.2016.7 Published online by Cambridge University Press

Comparison—toward a quantification of postdepositional *n*-alkane contamination

The comparison of the ^{14}C bulk *n*-alkane ages with the OSL ages (Fig. 1B) shows that within error the bulk *n*-alkanes of the three uppermost samples 15, 19, and 21 are well within the range or even slightly older than the OSL-inferred sedimentation ages for the LPS Gleina. This finding contradicts the thesis of a significant postdepositional *n*-alkane contamination by roots/rhizomicrobial OM in loess. Especially, for sample 15 where midchain length (i.e., C_{20}–C_{25}) compounds represent a dominant fraction, this finding has further implications. It may indicate either that the deposited charred biomass is of synsedimentary age or that microbial contribution of midchain *n*-alkanes was also synsedimentary and did not affect the radiocarbon age.

Only the lowermost *n*-alkane sample 23 is slightly younger than the OSL ages (Fig. 1B). As mentioned previously, an OSL age overestimation because of solifluction, cryo- or bioturbation, and incomplete signal resetting (i.e., partial bleaching) cannot be fully excluded for these sediments. Nevertheless, assuming that all OSL ages reflect sedimentation ages, it could be argued that sample 23 was contaminated postdepositionally by root/rhizomicrobial-derived *n*-alkanes and is therefore too young. In order to quantify the postdepositional contamination, we estimated for this sample the synsedimentary $F^{14}C$ value based on the (here interpolated) OSL age (42.3 ± 7.1 ka; Table 3) according to the following equation:

$$F^{14}C_{synsedimentary} = \left(\frac{1}{2}\right)^{\frac{t}{T\frac{1}{2}}} \quad \text{(Eq. 2)},$$

where *t* is the estimated uncalibrated ^{14}C age (assuming that OSL age equals calibrated ^{14}C age and using the intercept method and the IntCal13 calibration curve of Reimer et al. [2013]) and *T*½ is the half-life time of radiocarbon (5730 yr). In the same way, we estimated $F^{14}C$ for contaminating roots (Table 3). On the one hand, we hypothesize a more or less modern ($F^{14}C$ value of 1.0) or last-decadal *n*-alkane contamination by roots/rhizomicrobial deposition. Levin et al. (1985) observed atmospheric $F^{14}C$ values of more than 1.2 from 1962 to 1985 and up to almost 2.0 $F^{14}C$ in the year 1963 because of nuclear weapon tests in the Northern Hemisphere. An $F^{14}C$ value of 1.2 can be used to estimate the contamination that occurred during the last decades. On the other hand, we hypothesize a Holocene root/rhizomicrobial contamination and calculate according to Eq. 2 the theoretical $F^{14}C$ values for three Holocene time points (3 ka, 6 ka, and 9 ka; see Table 3). This is based on the finding of Gocke et al. (2010) and Pustovoytov and Terhorst (2004) that rhizoliths in last-glacial loess are of Holocene age.

The percentage of postdepositional *n*-alkane contamination "*x*" was then calculated using a ^{14}C isotope mass balance approach according to the following equation:

$$x\,\% = \frac{F^{14}C_{corrected} - F^{14}C_{synsedimentary}}{F^{14}C_{postsedimentary} - F^{14}C_{synsedimentary}} \quad \text{(Eq. 3)}.$$

Confidence intervals were calculated based on the $F^{14}C$ and OSL errors (Table 3). Accordingly, a modern and last-decadal

Table 3. ^{14}C isotope mass balance calculation for quantifying potential postdepositional contamination with root/rhizomicrobial-derived *n*-alkanes.

Sample name (depth in m)	Corrected $F^{14}C$	Sedimentation OSL age (ka)	Estimated uncalibrated synsedimentary ^{14}C ages[a] (ka)	Synsedimentary $F^{14}C$[b]	Suspected time of contamination (ka/cal ka BP)	Post-sedimentary $F^{14}C$	Percentage root/rhizomicrobial contamination	Error range based on $F^{14}C$ and OSL errors
					Modern	1.0000	3%	1%–5%
					Last decades	1.2000	2%	1%–4%
Sample 23 (9.8)	0.0391 ± 0.0105	42.3 ± 7.1	38.1 (31.4–45.9)	0.0100 (0.0039–0.0220)	3.0/3.2	0.6957	4%	1%–7%
					6.0/6.9	0.4839	6%	1%–10%
					9.0/10.1	0.3366	9%	2%–14%

[a]Assuming that optically stimulated luminescence (OSL) age equals calibrated ^{14}C age and using the intercept method and the IntCal13 calibration curve (Reimer et al., 2013).
[b]Calculated according to Eq. 2.

https://doi.org/10.1017/qua.2016.7 Published online by Cambridge University Press

root/rhizomicrobial *n*-alkane contamination of 3% (confidence interval 1%–5%) or a Holocene contamination of up to 9% (confidence interval 2%–14%) cannot be fully excluded for this particular sample (sample 23).

It should be mentioned that all radiocarbon ages are relatively close to their methodological age limit, and that the error bars are therefore relatively large. Nevertheless, our results lend further support to suggest that long-chain *n*-alkanes are not significantly contaminated by postdepositional OM. This is in agreement with findings from Häggi et al. (2014) based on compound-specific ^{14}C dating of *n*-alkanes (and long-chain *n*-alkanoic acids) in the LPS Crvenka, Serbia. Haas et al. (2016) also reported good agreement of ^{14}C ages from bulk *n*-alkanes with luminescence ages for the LPS Kurtak, central Siberia. It may thus not be necessary in all cases to do compound-specific radiocarbon dating, which is very laborious and requires specialized equipment and large amounts of samples. Dating bulk *n*-alkanes (i.e., at the compound-class level) probably has great potential for future loess-paleosol research.

CONCLUSIONS

For the investigated LPS Gleina, three out of four ^{14}C bulk *n*-alkane ages are well within the range or even slightly older than the OSL-inferred sedimentation ages. Only the fourth and lowermost sample may contain in absolute worst-case scenarios up to 5% of modern/last-decadal root-derived *n*-alkanes or up to 14% of Holocene root-derived *n*-alkanes based on ^{14}C isotope mass balance calculations. Our results show that (i) *n*-alkane biomarkers at our study site are not significantly contaminated by depositional OM, (ii) short- and midchain *n*-alkanes also have a synsedimentary age, and (iii) ^{14}C dating of leaf wax–derived bulk *n*-alkanes in loess-paleosols has great potential as a complementary dating tool for Quaternary research. More comparative bulk $^{14}C_{n\text{-alkane}}$ and OSL dating studies should be performed at other study sites, ideally also covering younger loess-paleosol deposits (i.e., not so close to the radiocarbon dating limits).

The results of our study suggest that in suitable LPSs, the contamination of older deposits with younger carbon is not a significant contributor to the carbon budget of the sediments. However, such an observation should be determined empirically for each study site to exclude the possibility of postdepositional movement of young carbon into older sediments.

ACKNOWLEDGMENTS

We are very grateful for constructive discussions and comments from B. Buggle, E. Lehndorff, J. Rethemeyer, and two anonymous reviewers on an earlier version of this manuscript. Part of these comments including our replies is available in an online discussion forum at http://www.biogeosciences-discuss.net/bg-2012-310/#discussion. Furthermore, we greatly acknowledge the constructive reviews and feedback provided by T. Reimann, the Associate Editor M. Lachniet, the Senior Editor N. Lancaster, and an anonymous reviewer, which helped to improve this manuscript. Prof. B. Huwe and Prof. L. Zöller generously provided laboratory facilities. We thank M. Sroka for support of the laboratory work and A. Kadereit from the Luminescence Laboratory of Heidelberg for her cooperation and making more machine time available.

This study was funded by the German Research Foundation (DFG; FA 239/13-2 and ZE 844/1-1). The work of S. Kreutzer and M. Fuchs was gratefully funded by the DFG (FU 417/7-2). M. Zech and R. Zech also gratefully acknowledge the support provided by the Alexander von Humboldt-Foundation and the Swiss National Foundation (SNF 131670 and SNF 150590), respectively.

Supplementary Materials

To view supplementary material for this article, please visit https://doi.org/10.1017/qua.2016.7

REFERENCES

Antoine, P., Rousseau, D.-D., Degeai, J.-P., Moine, O., Lagroix, F., Kreutzer, S., Fuchs, M., *et al*., 2013. High-resolution record of the environmental response to climatic variations during the last interglacial-glacial cycle in Central Europe: the loess-palaeosol sequence of Dolní Věstonice (Czech Republic). *Quaternary Science Reviews* 67, 17–38.

Bai, Y., Fang, X., Nie, J., Wang, Y., Wu, F., 2009. A preliminary reconstruction of the paleoecological and paleoclimatic history of the Chinese Loess Plateau from the application of biomarkers. *Palaeogeography, Palaeoclimatology, Palaeoecology* 271, 161–169.

Bronk Ramsey, C., 2009. Bayesian analysis of radiocarbon dates. *Radiocarbon* 51, 337–360.

Buggle, B., Wiesenberg, G.L.B., Glaser, B., 2010. Is there a possibility to correct fossil *n*-alkane data for postsedimentary alteration effects? *Applied Geochemistry* 25, 947–957.

Eglinton, G., Hamilton, R., 1967. Leaf epicuticular waxes. *Science* 156, 1322–1334.

Eglinton, T., Eglinton, G., 2008. Molecular proxies for paleoclimatology. *Earth and Planetary Science Letters* 275, 1–16.

Frechen, M., 2011. Loess in Eurasia. *Quaternary International* 234, 1–3.

Fuchs, M., Straub, J., Zöller, L., 2005. Residual luminescence signals of recent river flood sediments: a comparison between quartz and feldspar of fine- and coarse-grain sediments. *Ancient TL* 23, 25–30.

Gocke, M., Kuzyakov, Y., Wiesenberg, G.L.B., 2010. Rhizoliths in loess – evidence for post-sedimentary incorporation of root-derived organic matter in terrestrial sediments as assessed from molecular proxies. *Organic Geochemistry* 41, 1198–1206.

Gocke, M., Kuzyakov, Y., Wiesenberg, G.L.B., 2013. Differentiation of plant derived organic matter in soil, loess and rhizoliths based on *n*-alkane molecular proxies. *Biogeochemistry* 112, 23–40.

Gocke, M., Peth, S., Wiesenberg, G., 2014. Lateral and depth variation of loess organic matter overprint related to rhizoliths—revealed by lipid molecular proxies and X-ray tomography. *Catena* 112, 72–85.

Gocke, M., Wiesenberg, G.L.B., 2013. Interactive comment on "On the stratigraphic integrity of leaf-wax biomarkers in loess-paleosols" by C. Häggi *et al*. *Biogeosciences Discussions* 10, C7498–C7501.

Grimalt, J., Albaigés, J., 1987. Sources and occurrence of C_{12}-C_{22} *n*-alkane distributions with even carbon-numbered preference in sedimentary environments. *Geochimica et Cosmochimica Acta* 51, 1379–1384.

Haas, M., Bliedtner, M., Borodynkin, I., Salazar, G., Szidat, S., Eglinton, T., Zech, R., 2016. Radiocarbon dating of leaf waxes in the loess-paleosol sequence Kurtak, Central Siberia. Radiocarbon (in press).

Haase, G., Lieberoth, I., Ruske, R., 1970. Sedimente und Paläoböden im Lößgebiet. In Richter, H., Haase, G., Lieberoth, I., Ruske, R. (Eds.), *Periglazial - Löß - Paläolithikum im Jungpleistozän der Deutschen Demokratischen Republik*. VEB Hermann Haack, Gotha, Germany, pp 99–212.

Häggi, C., Zech, R., McIntyre, C., Zech, M., Eglinton, T.I., 2014. On the stratigraphic integrity of leaf-wax biomarkers in loess paleosols. *Biogeosciences* 11, 2455–2463.

Huang, Y., Li, B., Bryant, C., Bol, R., Eglinton, G., 1999. Radiocarbon dating of aliphatic hydrocarbons: a new approach for dating passive-fraction carbon in soil horizons. *Soil Science Society of America Journal* 63, 1181–1187.

Kadereit, A., Kind, C.-J., Wagner, G.A., 2013. The chronological position of the Lohne Soil in the Nussloch loess section – re-evaluation for a European loess-marker horizon. *Quaternary Science Reviews* 59, 67–86.

Kirkels, F., Jansen, B., Kalbitz, K., 2013. Consistency of plant-specific *n*-alkane patterns in plaggen ecosystems: a review. *Holocene* 23, 1355–1368.

Kolattukudy, P.E., 1976. Biochemistry of plant waxes. In Kolattukudy, P.E. (Ed.), *Chemistry and Biochemistry of Natural Waxes*. Elsevier, Amsterdam, pp 290–349.

Kreutzer, S., Fuchs, M., Meszner, S., Faust, D., 2012. OSL chronostratigraphy of a loess-palaeosol sequence in Saxony/Germany using quartz of different grain sizes. *Quaternary Geochronology* 10, 102–109.

Kuhn, T., Krull, E., Bowater, A., Grice, K., Gleixner, G., 2010. The occurrence of short chain *n*-alkanes with an even over odd predominance in higher plants and soils. *Organic Geochemistry* 41, 88–95.

Kusch, S., Rethemeyer, J., Schefuß, E., Mollenhauer, G., 2010. Controls on the age of vascular plant biomarkers in Black Sea sediments. *Geochimica et Cosmochimica Acta* 74, 7031–7047.

Lai, Z., Zöller, L., Fuchs, M., Brückner, H., 2008. Alpha efficiency determination for OSL of quartz extracted from Chinese loess. *Radiation Measurements* 43, 767–770.

Levin, I., Kromer, B., Schoch-Fischer, H., Bruns, M., Münnich, M., Berdau, D., Vogel, J.C., Münnich, K.O., 1985. 25 Years of tropospheric ^{14}C observations in Central Europe. *Radiocarbon* 27, 1–19.

Lichtfouse, E., Eglinton, T., 1995. ^{13}C and ^{14}C evidence of pollution of a soil by fossil fuel and reconstruction of the composition of the pollutant. *Organic Geochemistry* 23, 969–973.

Lieberoth, I., 1963. Lößsedimentation und Bodenbildung während des Pleistozäns in Sachsen. *Geologie* 12, 149–187.

Lisiecki, L.E., Raymo, M.E., 2005. A Pliocene-Pleistocene stack of 57 globally distributed benthic $\delta^{18}O$ records. *Paleoceanography* 20, PA1003. http://dx.doi.org/10.1029/2004PA001071.

Liu, W., Huang, Y., 2005. Compound specific D/H ratios and molecular distributions of higher plant leaf waxes as novel paleoenvironmental indicators in the Chinese Loess Plateau. *Organic Geochemistry* 36, 851–860.

Maffei, M., 1996. Chemotaxonomic significance of leaf wax alkanes in the Gramineae. *Biochemical Systematics and Ecology* 24, 53–64.

Marković, S.B., Catto, N., Smalley, I.J., Zöller, L., 2011. The second Loessfest (2009). *Quaternary International* 240, 1–3.

Marković, S.B., Stevens, T., Kukla, G.J., Hambach, U., Fitzsimmons, K.E., Gibbard, P., Buggle, B., *et al*., 2015. Danube loess stratigraphy—towards a pan-European loess stratigraphic model. *Earth-Science Reviews* 148, 228–258.

Mauz, B., Packman, S.C., Lang, A., 2006. The alpha effectiveness in silt-sized quartz: new data obtained by single and multiple aliquot protocols. *Ancient TL* 24, 47–52.

McDuffee, K., Timothy, E., Sessions, A., Sylva, S., Wagner, T., Hayes, J., 2004. Rapid analysis, of ^{13}C in plant-wax *n*-alkanes for reconstruction of terrestrial vegetation signals from aquatic sediments. *Geochemistry, Geophysics, Geosystems* 5, Q10004. http://dx.doi.org/10.1029/2004GC000772.

Meszner, S., Fuchs, M., Faust, D., 2011. Loess-Palaeosol-Sequences from the loess area of Saxony (Germany). *E&G Quaternary Science Journal* 60, 47–65.

Meszner, S., Kreutzer, S., Fuchs, M., Faust, D., 2013. Late Pleistocene landscape dynamics in Saxony, Germany: paleoenvironmental reconstruction using loess-paleosol sequences. *Quaternary International* 296, 94–107.

Murray, A.S., Wintle, A.G., 2000. Luminescence dating of quartz using an improved single-aliquot regenerative-dose protocol. *Radiation Measurements* 32, 57–73.

Nguyen Tu, T., Egasse, C., Zeller, B., Bardoux, G., Biron, P., Ponge, J.-F., David, B., Derenne, S., 2011. Early degradation of plant alkanes in soils: a litterbag experiment using ^{13}C-labelled leaves. *Soil Biology and Biochemistry* 43, 2222–2228.

Prescott, J.R., Hutton, J.T., 1994. Cosmic ray contributions to dose rates for luminescence and ESR dating: large depths and long-term time variations. *Radiation Measurements* 23, 497–500.

Pustovoytov, K., Terhorst, B., 2004. An isotopic study of a late Quaternary loess-paleosol sequence in SW Germany. *Revista Mexicana de Ciencias Geológicas* 21, 88–93.

Reimer, P.J., Bard, E., Bayliss, A., Beck, J.W., Blackwell, P.G., Bronk Ramsey, C., Buck, C.E., *et al*., 2013. IntCal13 and Marine13 radiocarbon age calibration curves 0–50,000 years cal BP. *Radiocarbon* 55, 1869–1887.

Schäfer, I., Bliedtner, M., Wolf, D., Faust, D., Zech, R., 2016. Evidence for humid conditions during the last glacial from leaf wax patterns in the loess-paleosol sequence El Paraíso, Central Spain. *Quaternary International* 407, 64–73.

Schäfer, I., Lanny, V., Franke, J., Eglinton, T., Zech, M., Vysloužilová, B., Zech, R., 2016. Leaf waxes in litter and topsoils along a European transect. *Soil* 2, 551–564.

Shah, S.R., Pearson, A., 2007. Ultra-microscale (5–25 μg C) analysis of individual lipids by ^{14}C AMS: assessment and correction for sample processing blanks. *Radiocarbon* 49, 69–82.

Stevens, T., Marković, S., Zech, M., Hambach, U., Sümegi, P., 2011. Dust deposition and climate in the Carpathian Basin over an independently dated last glacial–interglacial cycle. *Quaternary Science Reviews* 30, 662–681.

Wiesenberg, G., 2012. Interactive comment on "Technical note: *n*-alkane lipid biomarkers in loess: post-sedimentary or syn-sedimentary?" by M. Zech *et al*., *Biogeosciences Discussions* 9, C3541–C3545.

Wiesenberg, G.L.B., Gocke, M., 2013. Reconstruction of the late Quaternary paleoenvironments of the Nussloch loess paleosol sequence—comment to the paper published by Zech *et al.*, *Quaternary Research* 78, 2012, 226–235. Quaternary Research 79, 304–305.

Wiesenberg, G.L.B., Lehndorff, E., Schwark, L., 2009. Thermal degradation of rye and maize straw: lipid pattern changes as a function of temperature. *Organic Geochemistry* 40, 167–174.

Xie, S., Chen, F., Wang, Z., Wang, H., Gu, Y., Huang, Y., 2003. Lipid distributions in loess-paleosol sequences from northwest China. *Organic Geochemistry* 34, 1071–1079.

Xie, S., Wang, Z., Wang, H., Chen, F., An, C., 2002. The occurrence of a grassy vegetation over the Chinese Loess Plateau since the last interglacial: the molecular fossil record. *Science in China, Series D* 45, 53–62.

Zech, M., Andreev, A., Zech, R., Müller, S., Hambach, U., Frechen, M., Zech, W., 2010. Quaternary vegetation changes derived from a loess-like permafrost palaeosol sequence in northeast Siberia using alkane biomarker and pollen analyses. *Boreas* 39, 540–550.

Zech, M., Buggle, B., Leiber, K., Marković, S., Glaser, B., Hambach, U., Huwe, B., *et al.*, 2009. Reconstructing Quaternary vegetation history in the Carpathian Basin, SE-Europe, using *n*-alkane biomarkers as molecular fossils: problems and possible solutions, potential and limitations. *EG Quaternary Science Journal* 58, 148–155.

Zech, M., Krause, T., Meszner, S., Faust, D., 2013a. Incorrect when uncorrected: reconstructing vegetation history using *n*-alkane biomarkers in loess-paleosol sequences – a case study from the Saxonian loess region, Germany. *Quaternary International* 296, 108–116.

Zech, M., Kreutzer, S., Goslar, T., Meszner, S., Krause, T., Faust, D., Fuchs, M., 2012a. Technical note: *n*-alkane lipid biomarkers in loess: post-sedimentary or syn-sedimentary? *Biogeosciences Discussions* 9, 9875–9896. http://dx.doi.org/10.5194/bgd-9-9875-2012.

Zech, M., Pedentchouk, N., Buggle, B., Leiber, K., Kalbitz, K., Markovic, S., Glaser, B., 2011a. Effect of leaf litter degradation and seasonality on D/H isotope ratios of *n*-alkane biomarkers. *Geochimica et Cosmochimica Acta* 75, 4917–4928.

Zech, M., Rass, S., Buggle, B., Löscher, M., Zöller, L., 2012b. Reconstruction of the late Quaternary paleoenvironments of the Nussloch loess paleosol sequence, Germany, using *n*-alkane biomarkers. *Quaternary Research* 78, 226–235.

Zech, M., Tuthorn, M., Detsch, F., Rozanski, K., Zech, R., Zöller, L., Zech, W., Glaser, B., 2013c. A 220 ka terrestrial $\delta^{18}O$ and deuterium excess biomarker record from an eolian permafrost paleosol sequence, NE-Siberia. *Chemical Geology* 360–361, 220–230.

Zech, M., Zech, R., Buggle, B., Zöller, L., 2011b. Novel methodological approaches in loess research – interrogating biomarkers and compound-specific stable isotopes. *E&G Quaternary Science Journal* 60, 170–187.

Zech, R., Zech, M., Marković, S., Hambach, U., Huang, Y., 2013b. Humid glacials, arid interglacials? Critical thoughts on pedogenesis and paleoclimate based on multi-proxy analyses of the loess-paleosol sequence Crvenka, Northern Serbia. *Palaeogeography, Palaeoclimatology, Palaeoecology* 387, 165–175.

Zhang, Z., Zhao, M., Eglinton, G., Lu, H., Huang, C., 2006. Leaf wax lipids as paleovegetational and paleoenvironmental proxies for the Chinese Loess Plateau over the last 170 kyr. *Quaternary Science Reviews* 20, 575–594.

Zöller, L., Faust, D., 2009. Lower latitudes loess—dust transport past and present. *Quaternary International* 196, 1–3.

Zöller, L., Pernicka, E., 1989. A note on overcounting in alpha-counters and its elimination. *Ancient TL* 7, 11–14.

https://doi.org/10.1017/qua.2016.7 Published online by Cambridge University Press